

QED corrections to the big-bang nucleosynthesis reaction rates

Cyril Pitrou^{1,*} and Maxim Pospelov^{2,†}

¹*CNRS, UMR 7095, Institut d'Astrophysique de Paris, 98bis Bd Arago, 75014 Paris, France.*

²*Perimeter Institute for Theoretical Physics, Waterloo, ON N2J 2W9, Canada;*

Department of Physics and Astronomy, University of Victoria, Victoria, BC V8P 5C2, Canada.

We compute radiative corrections to nuclear reaction rates that determine the outcome of the Big-Bang Nucleosynthesis (BBN). Any nuclear reaction producing a photon with an energy above $2m_e$ must be supplemented by the corresponding reaction where the final state photon is replaced by an electron-positron pair. We find that pair production brings a typical 0.2% enhancement to photon emission rates, resulting in a similar size corrections to elemental abundances. The exception is ${}^4\text{He}$ abundance, which is insensitive to the small changes in the nuclear reaction rates. We also investigate the effect of vacuum polarisation on the Coulomb barrier, which brings a small extra correction when reaction rates are extrapolated from the measured energies to the BBN Gamow peak energies.

I. INTRODUCTION

Precise values of nuclear reaction rates are sometimes required in astrophysics and cosmology. While most of the applications belong to the stellar nucleosynthesis and solar neutrino physics, the one distinct cosmological application where precise nuclear physics is required is the Big-bang Nucleosynthesis (BBN). Developments of the last two decades, with an independent input of the baryon-to-photon ratio from the Cosmic Microwave Background (CMB) anisotropies, paired with advances in observational extraction of the deuterium and helium abundance [1–3], have contributed to the rise of the standard cosmological model of the Universe. Further progress in refinement of BBN may only come from the combination of advances in CMB, more precise observations of primordial abundances, and %-level determination of nuclear rates.

Quantitatively, the BBN has entered an era of precision, since errors of 1.6% (at one standard deviation) and smaller on ${}^4\text{He}$ [3, 4] have been claimed in recent years. At the same time, one should be cautious recognizing that it is very difficult to correctly estimate all systematic errors in helium abundance measurements, hence such a precision must not be taken at face value. Furthermore, current measurements of deuterium abundances [2] have reached an unprecedented 1.2% precision. The total yield of ${}^4\text{He}$ is essentially set by the neutron-to-proton ratio at the time of BBN that is mainly controlled by the weak interaction rates, while the feedback from other elements is small. Many subtle effects, including radiative corrections, have been taken into account in Refs. [5–9], and reviewed in Ref. [10], to reach a 0.1% theoretical precision on the weak rates. At the moment, the main source of theoretical uncertainty in the weak rates is the neutron lifetime which is used as a proxy to estimate the strength of the weak interactions. The incomplete decoupling of

neutrinos prior to the reheating of photons by electrons-positrons annihilations leads to a slight modification of the energy density in neutrinos [11–14], which in turn affects the neutron abundance via the modification of the Hubble expansion rate and flavour-specific distortions of the overall neutrino abundance.

Only traces amounts of other elements are left at the end of BBN, and their final abundances depend on the nuclear rates of a limited network of reactions, typically a dozen. The most relevant nuclei produced during BBN are deuterium (D), ${}^3\text{He}$, ${}^3\text{H}$, ${}^7\text{Li}$ and ${}^7\text{Be}$ ¹. Reaching a percent level predictions for key nuclear reactions is highly desirable in the context of precise BBN predictions for these elements. In most cases, direct measurement of the reaction rate in experiment is performed, with some key reaction rates now being known down to $\approx 5\%$ accuracy. A theoretical *ab-initio* approach has also been successful. For a long time, theory determination of $n+p \leftrightarrow \text{D} + \gamma$ rate has been more accurate than the corresponding experimental measurement (see, *e.g.* Ref. [15] for the nuclear effective theory approach to this rate), and the corresponding errors are at a sub-% percent level. A significant theoretical progress has also been achieved in more complicated rates such as $\text{D} + p$ and $\text{D} + n$ fusion processes [16], $\text{D} + \text{D}$ reactions [17], ${}^3\text{H} + \text{D} \leftrightarrow n + {}^4\text{He}$ and ${}^3\text{He} + \text{D} \leftrightarrow p + {}^4\text{He}$ reactions [18], ${}^3\text{He} + {}^4\text{He} \leftrightarrow {}^7\text{Be} + \gamma$ and ${}^3\text{H} + {}^4\text{He} \leftrightarrow {}^7\text{Li} + \gamma$ reactions [19, 20].

Until now, the radiative corrections to nuclear rates have been ignored in the compilation of the BBN reaction networks. The goal of the current paper is to give a quantitative assessment of radiative corrections to the nuclear BBN rates, and determine the resulting shift in the yield for the main elements. There are two types of contributions that we need to consider: *i.* Replacement of an on-shell photon with a lepton pair, *ii.* Virtual excitation of the electron-positron vacuum, modifying the

*pitrou@iap.fr

†mpospelov@perimeterinstitute.ca

¹ ${}^7\text{Be}$ decays subsequently to ${}^7\text{Li}$, and ${}^3\text{H}$ to ${}^3\text{He}$. It is customary to report the final abundances of ${}^7\text{Li}$ and ${}^3\text{He}$ as their direct production augmented by these decay products.

Coulomb interaction of nuclei. There are several simplifying conditions that would allow us to perform this evaluation *without* having to treat unknown nuclear matrix elements. Such conditions include a possibility of making a reliable multipole expansion, as the wavelengths of real/virtual photons are much larger than the characteristic nuclear size, $\lambda_\gamma \gg R_N$. The second simplifying condition is that the kinetic energies of incoming particles participating in the reactions are much smaller than the characteristic Gamow energies, $E \ll E_G$ (or equivalently, $Z_1 Z_2 e^2 / (\hbar v) \gg 1$, where v is relative velocity and $Z_{1(2)}e$ are charges of the reactants), and all reactions occur in the Coulomb-suppressed regime.

An important class of BBN reactions involves a on-shell photon, with energy $E_\gamma > 2m_e$. Then, there exists a reaction where this photon is virtual, and decays into a lepton pair [21, 22]. In other words, instead of a reaction $N_1 + N_2 \rightarrow N_3 + \gamma$, one could always have $N_1 + N_2 \rightarrow N_3 + e^+ e^-$ reaction. Importantly, for reactions in which the cross section is measured by detection of the real photon, this extra channel is necessarily ignored and the inclusion of the final state pair will raise the total $N_1 + N_2 \rightarrow N_3$ rate. We shall evaluate in section II this correction for the rates

$$n + p \rightarrow D + \gamma, \quad (1a)$$

$$p + D \rightarrow {}^3\text{He} + \gamma, \quad (1b)$$

$${}^3\text{H} + {}^4\text{He} \rightarrow {}^7\text{Li} + \gamma, \quad (1c)$$

$${}^3\text{He} + {}^4\text{He} \rightarrow {}^7\text{Be} + \gamma, \quad (1d)$$

$${}^3\text{H} + p \rightarrow {}^4\text{He} + \gamma. \quad (1e)$$

Notice that for ${}^7\text{Be} + p \rightarrow {}^8\text{B} + \gamma$ reaction, not relevant for BBN (but important for *e.g.* solar neutrino physics), the energy release is not sufficient to produce a pair. In principle, there are also various cross channels for these reactions, $N_3 + e^+ e^- \rightarrow N_1 + N_2$, and $N_3 + e^\pm \rightarrow N_1 + N_2 + e^\pm$. In practice, these are going to be less important than the electron-positron production reactions, because at most relevant temperatures, $T < 100$ keV, the abundance of electrons and positrons in the thermal bath is quite small.

Insertion of electron-positron loop inside a virtual photon is another way the radiative corrections tend to manifest themselves. For a nuclear reaction among charged particles at $E \ll E_G$, the Coulomb repulsion is very important. In the static approximation, this radiative effect modifies the Coulomb potential to what is known as the Uehling-Serber potential [23–25]. This potential - rather than a simple Coulomb r^{-1} form - should be used in calculating the penetration factors. If the cross sections are measured at exactly the same range of energies relevant for the BBN reactions (*i.e.* Gamow peak energies), then the effect of Uehling-Serber potential is already accounted for in the measured cross section. If, however, one needs to extrapolate nuclear rates in energy (from the energy of the measurement to the Gamow peak) and precision is required, such an extrapolation must be done using the expression for the penetration factors in the Uehling-Serber potential. In the following, we shall con-

sider how this effect modifies the penetration factor of the key reaction (1b) (section III).

Note that in principle there are additional types of radiative corrections. For instance bremsstrahlung from one of the charged reacting nuclei may in principle be taken into account. However, for a nucleus with non-relativistic kinetic energy E_K and mass M , such an effect is typically suppressed not only by the fine structure constant α_{FS} but also by powers of E_K/M . Similar suppressions would apply to any additional “structural” photons, emitted from the nuclear transitions inside a nuclear reaction. With typical kinetic energies (MeV of sub-MeV) this can be safely disregarded.

Finally, the implications for the freeze-out elemental abundances at the end of BBN are given in section IV.

II. PAIR PRODUCTION REACTIONS

A. Notation

We review in detail the pair production corrections to reaction (1a), because we want to compare the relative importance of the photon and the pair producing reactions

$$n + p \rightarrow D + \gamma, \quad (2a)$$

$$n + p \rightarrow D + e^+ + e^-. \quad (2b)$$

Throughout we use the particle physics metric signature $(+, - - -)$. We denote the electron and positron momenta p_1 and p_2 , the deuterium momentum is P' , and the sum of the initial neutron and proton momenta is P . The electron, proton, neutron and deuterium masses are respectively m , m_p , m_n , m_D . The average nucleon mass is taken to be $m_N \equiv (m_n + m_p)/2$. k is either the photon momentum or the sum of the electron and positron momenta ($k = p_1 + p_2$), depending on the reaction considered, such that in all cases from momentum conservation one has $P = P' + k$. Finally, ϵ^μ is the photon polarization vector. Throughout our calculations we put \hbar and c to one.

B. E -type and B -type transitions

We work in the Coulomb gauge for which the vector potential is only spatial for a reference observer whose four-velocity is u , that is $\epsilon \cdot u = 0$. In the rest frame of the reference observer, $u^\mu = \delta_0^\mu$ and we split the photon momentum (be it real or virtual) into frequency and spatial momentum as $k^\mu = (\omega, q^i)$, that is $k \cdot u = \omega$. In practice, we use the center-of-mass rest frame to define the reference observer. We further define the magnitude of the photon wave-vector q and its direction n^i , that is $q^i = q n^i$ with $\mathbf{n} \cdot \mathbf{n} = 1$. The transition matrix of the γ reaction is necessarily of the form

$$\mathcal{M} = \mathcal{J}_\mu \epsilon^\mu = \mathcal{J}_i \epsilon^i, \quad (3)$$

where $\mathcal{J}_\mu \equiv (\mathcal{J}_0, \mathcal{J}_i)$ is the nuclear transition current. Given gauge invariance, it satisfies the transverse condition

$$\mathcal{J}_\mu k^\mu = 0 \quad \Rightarrow \quad \mathcal{J}_i q^i = \omega \mathcal{J}_0. \quad (4)$$

We now consider that \mathcal{J}_μ can be expanded in powers of $\omega/|\mathbf{p}_N|$ (or $q/|\mathbf{p}_N|$), where \mathbf{p}_N is the typical spatial momentum of the nucleons inside deuterium. This amounts to assuming that the typical wavelength of photons $2\pi/\omega$ is much larger than the typical size of the deuterium nucleus $\propto 1/|\mathbf{p}_N|$. Since $|\mathbf{p}_N| \approx \sqrt{2m_D B_D}$, where B_D is the deuterium binding energy, and the typical energy of the emitted photon is B_D , our expansion is in fact in powers of $\sqrt{B_D}/(2m_D) \approx 0.025$. At lowest order in this expansion, \mathcal{J}_i can be separated into electric and magnetic dipole contributions as

$$\mathcal{J}_i = \mathcal{E}_i + \mathcal{B}_i, \quad (5)$$

$$\mathcal{E}_i = \omega d_i, \quad (6a)$$

$$\mathcal{B}_i = \epsilon_{jki} m^j q^k, \quad (6b)$$

in which d_i (resp. m_i) is the electric (resp. magnetic) dipole of the nuclear transition. Note that by construction $\mathcal{J}_0 = d_i q^i$ and $\mathcal{B}_i q^i = 0$. Eqs. (6) can be recast in covariant form as

$$\mathcal{E}_\mu = -(k \cdot u) d_\mu + (d \cdot k) u_\mu, \quad (7a)$$

$$\mathcal{B}_\beta = u^\mu m^\nu \epsilon_{\mu\nu\alpha\beta} k^\alpha. \quad (7b)$$

Physically, this is equivalent to considering either a coupling to the Faraday tensor polarisation or its dual, since

$$\mathcal{E}_\mu \epsilon^\mu = d_\mu u_\nu F^{\mu\nu}, \quad F^{\mu\nu} \equiv k^\mu \epsilon^\nu - k^\nu \epsilon^\mu, \quad (8a)$$

$$\mathcal{B}_\beta \epsilon^\beta = \frac{1}{2} u^\mu m^\nu \epsilon_{\mu\nu\alpha\beta} F^{\alpha\beta} = u^\mu m^\nu \tilde{F}_{\mu\nu}. \quad (8b)$$

When averaging over all spins and directions, results can only depend on the magnitude of momenta. Hence we can always replace

$$d^\mu d^\nu \rightarrow -\frac{1}{3} |d|^2 (g^{\mu\nu} - u^\mu u^\nu) \quad (9)$$

or $d^i d^j \rightarrow |d|^2 \delta^{ij}/3$, where $|d|^2 \equiv -(d \cdot d)$. We use a similar property and definitions for the magnetic dipole. We use this arrow notation whenever the expression is reduced using this angular average.

C. Photon producing reaction

If we now compute $|\mathcal{M}|^2$ for the photon process, we get

$$|\mathcal{M}^2|_{(\gamma)} = \sum_{s=\pm 1} \mathcal{J}_\mu \mathcal{J}_\nu^* \epsilon_s^\mu \epsilon_s^{\nu*} = -g^{\mu\nu} \mathcal{J}_\mu \mathcal{J}_\nu^*. \quad (10)$$

With minimal algebra we find

$$|\mathcal{M}|_{(\gamma),\mathcal{E}}^2 \rightarrow \frac{2|d|^2}{3} |\mathbf{q}|^2, \quad (11a)$$

$$|\mathcal{M}|_{(\gamma),\mathcal{B}}^2 \rightarrow \frac{2|m|^2}{3} |\mathbf{q}|^2, \quad (11b)$$

noting that the parity considerations prevent interference terms in the angularly averaged matrix elements.

D. Pair producing reaction

For the pair producing reaction, we treat $\mathcal{J}_\mu A^\mu$ as a vertex inside usual Feynman rules,

$$|\mathcal{M}|_{(ee)}^2 = \mathcal{J}_\mu \mathcal{J}_\nu^* T^{\mu\nu} \quad (12)$$

where

$$\begin{aligned} T^{\mu\nu} &\equiv \frac{e^2}{(k \cdot k)^2} (\not{k} + m_e) \gamma^\mu (\not{k} - m_e) \gamma^\nu, \\ &= \frac{e^2}{k^4} (-g^{\mu\nu} 2k^2 + 4p_1^\mu p_2^\nu + 4p_2^\mu p_1^\nu). \end{aligned} \quad (13)$$

Defining $E_1 = p_1 \cdot u$ and $E_2 = p_2 \cdot u$ and using angular averaging rules (9), we get

$$|\mathcal{M}|_{(ee),\mathcal{E}}^2 \rightarrow \frac{2|d|^2 e^2}{3k^4} [(E_1 + E_2)^2 (4m_e^2 + 2k^2) - 4k^2 E_1 E_2 + k^4], \quad (14a)$$

$$|\mathcal{M}|_{(ee),\mathcal{B}}^2 \rightarrow \frac{2|m|^2 e^2}{3k^4} \{4m_e^2 [(E_1 + E_2)^2 - k^2] - k^4 + 2k^2 [(E_1)^2 + (E_2)^2]\}. \quad (14b)$$

E. Ratio of rates

Ultimately, the cross sections of $n + p \rightarrow D$ fusion are corrected by

$$\sigma^{(\gamma)} \rightarrow \sigma^{(\gamma)} (1 + r) \quad (15)$$

where the ratio of the pair producing and photon producing rates is found from

$$r \equiv \frac{\sigma^{(ee)}}{\sigma^{(\gamma)}} = \frac{\int d^5 \Phi_{12D}}{\int d^2 \Phi_{\gamma D}}, \quad (16)$$

and is a function of reaction energy E_K . The phase-space elements are

$$\begin{aligned} d^5 \Phi_{12D} &\equiv (2\pi)^4 \delta^4(P - k - P') |\mathcal{M}|_{(ee)}^2 [dp_1][dp_2][dP'], \\ d^2 \Phi_{\gamma D} &\equiv (2\pi)^4 \delta^4(P - k - P') |\mathcal{M}|_{(\gamma)}^2 [dp_\gamma][dP'], \end{aligned}$$

with $[dp] \equiv d^3 \mathbf{p}/(2E_p)$. Since the electric and magnetic dipoles contribute separately, there is a ratio as defined in (16) for each case.

We choose to work in the center-of-mass frame in which $P^\mu = Eu^\mu$, where E is the total initial energy. Furthermore, we also use an infinite deuterium mass expansion. This is equivalent to expanding the results in a power series of $1/m_D$, by expressing all energies with respect to the deuterium mass, and then considering only the lowest order term in such expansion. Physically, it corresponds to ignoring deuterium recoil. Hence, in the photon producing case, the available energy E_a goes entirely in the emitted photon and we can use

$$\omega = q = E_a \equiv E - m_D = E_K + B_D. \quad (17)$$

where $E_K \equiv E - m_n - m_p$ is the center-of-mass kinetic energy of the initial neutron-proton pair.

The integral over phase space for the reference photon reaction is then simply

$$\int d^2\Phi_{\gamma D} = \frac{|\mathcal{M}|_{(\gamma)}^2 \omega}{4\pi m_D}. \quad (18)$$

As for the pair producing reactions we find

$$\begin{aligned} d^2\Phi_{12D} &\equiv \int_{\text{angles}} d^5\Phi_{12D} \\ &= \frac{|\mathcal{M}|_{(ee)}^2}{4(2\pi)^3(2E)^2} d(k^2) d(m_{2D}^2). \end{aligned} \quad (19)$$

where we used the invariant mass $m_{2D}^2 \equiv (p_2 + P')^2$. Integrating over the range of allowed values for this invariant mass, we find the differential ratios

$$\frac{dr_{\mathcal{E}}}{dk^2} = \left(1 + \frac{x}{2}\right) \frac{\alpha_{\text{FS}}}{6\pi} \sqrt{(1-x)(x-a)}(a+2x) \quad (20a)$$

$$\frac{dr_{\mathcal{B}}}{dk^2} = (1-x) \frac{\alpha_{\text{FS}}}{6\pi} \sqrt{(1-x)(x-a)}(a+2x) \quad (20b)$$

where

$$x \equiv k^2/E_a^2, \quad a \equiv 4m_e^2/E_a^2. \quad (21)$$

Further integrating on the allowed values $4m_e^2 \leq k^2 \leq E_a^2$ leads to

$$\begin{aligned} r_{\mathcal{E}} &= \frac{\alpha_{\text{FS}}}{9\pi\sqrt{a}} \left[-a(10+a)E(1-a^{-1}) \right. \\ &\quad \left. + (6 + \frac{7}{2}a + \frac{3}{2}a^2)K(1-a^{-1}) \right], \end{aligned} \quad (22a)$$

$$\begin{aligned} r_{\mathcal{B}} &= \frac{\alpha_{\text{FS}}}{9\pi\sqrt{a}} \left[a(-13+5a)E(1-a^{-1}) \right. \\ &\quad \left. + (6+5a-3a^2)K(1-a^{-1}) \right]. \end{aligned} \quad (22b)$$

In these expressions, E is the complete elliptic integral of the second kind, and K is the complete elliptic integral of the first kind².

² These integrals are defined by $E(m) = \int_0^{\pi/2} (1 - m \sin^2 \theta)^{1/2} d\theta$ and $K(m) = \int_0^{\pi/2} (1 - m \sin^2 \theta)^{-1/2} d\theta$.

F. Analytic approximation of ratios

In addition to the infinite deuterium mass approximation, one can also consider a limit of energy release being much larger than the electron mass, $E_a \gg m_e$. Expanding expressions from previous subsections in small $2m_e/E_a$, we arrive at

$$r_{\mathcal{E}} \approx \frac{2\alpha_{\text{FS}}}{3\pi} \left[\ln(2E_a/m_e) - \frac{5}{3} \right], \quad (23a)$$

$$r_{\mathcal{B}} \approx \frac{2\alpha_{\text{FS}}}{3\pi} \left[\ln(2E_a/m_e) - \frac{13}{6} + \frac{9m_e^2}{2E_a^2} \right]. \quad (23b)$$

These approximations, along with the result of the direct numerical integration of (16) without using the infinite deuterium mass approximation, are depicted in Fig. 1. Note that the leading logarithmic terms in (23a) and (23b) has the same coefficient. It is model-independent, because the answer for the pair-production in this limit is dominated by a quasi-real photon.

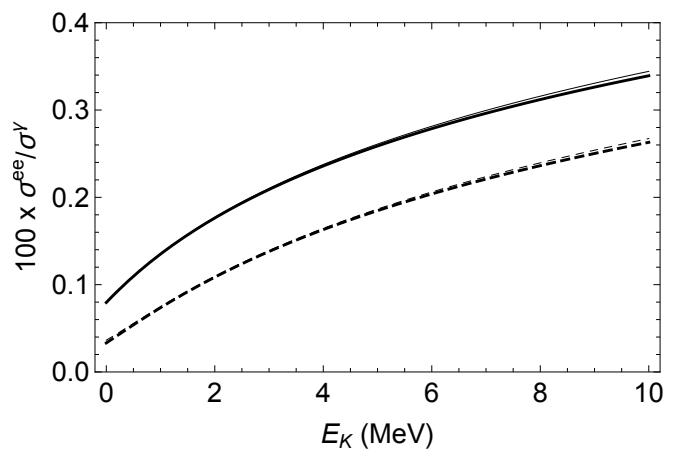


FIG. 1: Solid is electric dipole ratio, dashed is magnetic dipole ratio. The result of the full numerical integration of (16) without approximation is depicted in thick lines, and the analytic approximations (23a) and (23b) are in thin lines.

G. Comparison with literature

Our results can be compared with the approach of [21]. However note that in this reference, a factor 2 is missing in front of the last term of Eq. (6), hence there is a missing factor 2 in front of the R_L term in its Eq. (9). The validity of Eq. (9) in [21] is restored if one alters the definition of R_L by adding an extra factor 2.

With this convention, we follow [21] in defining the

transverse and longitudinal components of the ratios as

$$R_T \equiv \frac{\int d^2\Omega_{\hat{k}} \mathcal{J}_i^{(ee)} \mathcal{J}_j^{(ee)} (\delta^{ij} - \hat{k}^i \hat{k}^j)}{\int d^2\Omega_{\mathbf{n}} \mathcal{J}_i^{(\gamma)} \mathcal{J}_j^{(\gamma)} (\delta^{ij} - n^i n^j)} \quad (24a)$$

$$R_L \equiv 2 \frac{\int d^2\Omega_{\hat{k}} \mathcal{J}_i^{(ee)} \mathcal{J}_j^{(ee)} \hat{k}^i \hat{k}^j}{\int d^2\Omega_{\mathbf{n}} \mathcal{J}_i^{(\gamma)} \mathcal{J}_j^{(\gamma)} (\delta^{ij} - n^i n^j)} \quad (24b)$$

where \hat{k}^i is the unit vector in the direction of the spatial momentum of the virtual photon.

Our modeling (7) of the electric and magnetic dipoles corresponds in the infinite deuterium mass approximation to

$$R_T^{\mathcal{E}} = 1, \quad R_L^{\mathcal{E}} = 1, \quad (25)$$

$$R_T^{\mathcal{B}} = \left(\frac{|\mathbf{p}_1 + \mathbf{p}_2|}{\omega} \right)^2, \quad R_L^{\mathcal{B}} = 0, \quad (26)$$

and from kinematics $|\mathbf{p}_1 + \mathbf{p}_2|/\omega = \sqrt{1-x}$ in the notation (21).

It is found in Eq. (10) of [21], that the subleading constant for $R_T = 1$ and $R_L = 0$ is $-11/6$ [in units of $2\alpha_{\text{FS}}/(3\pi)$]. Since our electric dipole parameterisation contributes to $R_L^{\mathcal{E}} = 1$, it brings a subleading constant contribution, hence the slightly different constant $-5/3$ found in (23a). Furthermore the subleading constant in (23b) is also different from $-11/6$, even though $R_L^{\mathcal{B}} = 0$, due to the non-constancy of $R_T^{\mathcal{B}}$ in our magnetic dipole parameterisation.

Note that more generally, if $R_T = C_T(|\mathbf{p}_1 + \mathbf{p}_2|/\omega)^p$ and $R_L = C_L(|\mathbf{p}_1 + \mathbf{p}_2|/\omega)^q$, the differential ratio is

$$\frac{dr}{dk^2} = \left[C_T(1-x)^{p/2} + C_L \frac{x}{2}(1-x)^{q/2} \right] \times \frac{\alpha_{\text{FS}}}{6\pi} \sqrt{(1-x)(x-a)(a+2x)}. \quad (27)$$

H. Reference rates

It is well known that in the $n + p \rightarrow \text{D} + \gamma$ reaction, at low energy the contribution of the magnetic channel is enhanced due to the virtual state close to threshold. Therefore, in order to know what the absolute correction of the BBN rates due to pair-production is, one needs to know how $\sigma_{(\gamma)}$ splits into the electric and magnetic components. While this calculation has been treated in considerable detail over the years, we would use a simplified approach of ‘‘zero range approximation’’ for the nuclear potential (see *e.g.* section 58 of [26]), that results in $\sigma_{(\gamma)}$ within 10% from a more accurate answer.

Photo-dissociation rates are the sum of electric and magnetic dipole contributions

$$\sigma^{\text{D}+\gamma \rightarrow n+p} = \sigma_{\mathcal{E}}^{\text{D}+\gamma \rightarrow n+p} + \sigma_{\mathcal{B}}^{\text{D}+\gamma \rightarrow n+p} \quad (28)$$

where [Eqs. 58.4-58.7 of [26]]

$$\sigma_{\mathcal{E}}^{\text{D}+\gamma \rightarrow n+p} = \frac{8\pi\alpha_{\text{FS}} \sqrt{B_{\text{D}}}(\omega - B_{\text{D}})^{3/2}}{3m_N \omega^3} \quad (29a)$$

$$\sigma_{\mathcal{B}}^{\text{D}+\gamma \rightarrow n+p} = \frac{8\pi}{3}(\mu_p - \mu_n)^2 \times \frac{\sqrt{B_{\text{D}}}(\omega - B_{\text{D}})(\sqrt{B_{\text{D}}} + \sqrt{E_{s=0}})^2}{\omega(\omega - B_{\text{D}} + E_{s=0})^2} \quad (29b)$$

with $E_{s=0} \approx 0.067$ MeV the energy of the unstable spin zero state of deuterium. The proton and neutron magnetic moments are $\mu_p = 2.793\mu_N$ and $\mu_n = -1.913\mu_N$ where the nuclear Bohr magneton can be written as $\mu_N \equiv \sqrt{\alpha_{\text{FS}}}/(2m_p)$.

From detailed balance, they are related to the corresponding fusion rates by

$$\frac{\sigma_{\mathcal{E}/\mathcal{B}}^{n+p \rightarrow \text{D}+\gamma}}{\sigma_{\mathcal{E}/\mathcal{B}}^{\text{D}+\gamma \rightarrow n+p}} = \frac{3\omega^2}{2m_N(\omega - B_{\text{D}})}. \quad (30)$$

The cross sections for the reactions with pair production are estimated using (22a) and (22b):

$$\sigma_{\mathcal{E}/\mathcal{B}}^{(ee)} \approx r_{\mathcal{E}/\mathcal{B}} \times \sigma_{\mathcal{E}/\mathcal{B}}^{n+p \rightarrow \text{D}+\gamma}. \quad (31)$$

I. Average over thermal distributions

In a thermalised plasma, the cross section must be averaged over the thermal distribution of relative velocities between neutrons and protons in order to obtain interaction rates. The general expression is

$$\langle \sigma v \rangle = \frac{2}{\sqrt{\pi T^3}} \int \sigma(E_K) v_{\text{rel}}(E_K) e^{-E_K/T} \sqrt{E_K} dE_K \quad (32)$$

where $v_{\text{rel}}(E_K) = \sqrt{2E_K/\mu}$, with μ the reduced mass of the reacting nuclei which for neutrons and protons forming deuterium is approximately $m_N/2$.

Performing the thermal average of reference rate $\langle \sigma v \rangle^{(\gamma)}$ by applying (32) to Eqs. (29a) and (29b), we observe a rather good agreement with results of Ref. [15], especially at low energies. Combining the reference cross section [(30) with (29)] with the corrective factors (22) as specified by (31), we are in position to estimate the magnitude of the pair production corrections to the rates. The results are depicted in Fig. 2. A fitting formula in the range $0.05 < T_9 < 5$ is

$$\frac{\langle \sigma v \rangle^{(\gamma)} + \langle \sigma v \rangle^{(ee)}}{\langle \sigma v \rangle^{(\gamma)}} = 1 + \sum_{i=0}^4 a_i T_9^i \quad (33)$$

where T_9 is the temperature in GK and $a_0 = 3.6367 \times 10^{-4}$, $a_1 = 9.0830 \times 10^{-5}$, $a_2 = 4.1675 \times 10^{-5}$, $a_3 = -1.1675 \times 10^{-5}$ and $a_4 = 1.0263 \times 10^{-6}$.

It is easy to see that, at high temperatures, the relative size of the correction is sub-%, while at lower temperatures, where magnetic transition dominates, it drops to below the 10^{-3} level.

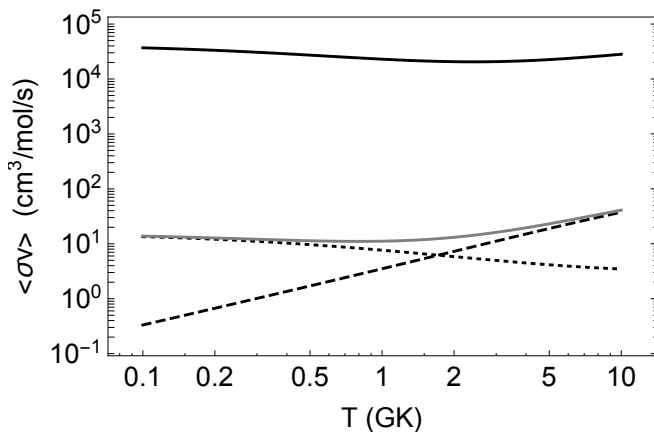


FIG. 2: The electric (resp. magnetic) dipole contribution to $\langle\sigma v\rangle^{(ee)}$ is in dashed line (resp. dotted line). The total correction is shown by the gray line while the reference value for $\langle\sigma v\rangle^{(\gamma)}$ (based on Eqs. (29)) is in solid.

J. Pair production for other reactions

For all other reactions, the magnetic dipole contribution is subdominant. However, for the $p + D \rightarrow {}^3\text{He} + \gamma$ reaction, the magnetic dipole contribution is only marginally subdominant since it contributes around 15% at BBN energies (see table 3 of Ref. [27]). Given the size of the corrections reported in table I and the similarities between the electric and dipole corrections [Eqs. (23)] when the energy release exceeds $Q \gg 2m_e$, we ignore this detail which would only bring a small correction to the already small correction. Hence, knowing the cross section for the photon emission reaction, we just need to multiply it by the electric dipole corrective factor (22a) to get to the pair-production rate. An important subtlety is that the pair-production correction needs to be applied to rates that had their cross sections measured via the detection of photon. The cross section of the reaction of $p + D \rightarrow {}^3\text{He} + \gamma$ is a prime example of that, because it is measured via the final photon [28–30]. This also applies to reaction ${}^3\text{H} + p \rightarrow {}^4\text{He} + \gamma$ in Ref. [31], and to the most precise measurements of ${}^3\text{H} + {}^4\text{He} \rightarrow {}^7\text{Li} + \gamma$ reaction [32].

On the other hand, recommended reaction rates for the ${}^3\text{He} + {}^4\text{He} \rightarrow {}^7\text{Be} + \gamma$ are based on the resulting ${}^7\text{Be}$ activity in order to keep statistics of the fits tractable [33, 34]. Therefore, the total rate is measured, including the radiative correction. Hence, we should not include the pair production correction to the reaction ${}^3\text{He} + {}^4\text{He} \rightarrow {}^7\text{Be} + \gamma$.

Furthermore, since we are interested in corrections to the thermally averaged rates, one should in principle estimate the correction to the thermally averaged rates by applying (32) to the corrected cross-sections. Given the size of the corrections, we find it sufficient to multiply the thermally averaged rates of the photon producing reactions by the corrective ratios (22a) evaluated at

the most relevant kinetic energy for a given temperature and reaction (*i.e.* Gamow peak energy). For two nuclei with Z_1 and Z_2 proton number and reduced mass $\mu = uA_1A_2/(A_1 + A_2)$, it is given (see Ref. [35]) by

$$E_K^{\text{ML}}(T_9) \approx \left(\frac{\mu}{2}\right)^{1/3} (\pi\alpha_{\text{FS}}Z_1Z_2k_B T)^{2/3} \\ \approx 0.1220(\mu/u)^{1/3}(Z_1Z_2T_9)^{2/3} \text{ MeV}. \quad (34)$$

For the photon emission reactions relevant for BBN, the corrections at $T_9 = 0.8$ are reported in Table I. Evidently it affects mostly reactions with larger Q values, since a larger available energy brings larger values for the logarithms of Eq. (23a).

Reaction	Q in MeV	Correction (in %)
$p + D \rightarrow {}^3\text{He} + \gamma$	5.493	0.220
${}^3\text{H} + {}^4\text{He} \rightarrow {}^7\text{Li} + \gamma$	2.468	0.106
${}^3\text{He} + {}^4\text{He} \rightarrow {}^7\text{Be} + \gamma$	1.587	0.057
${}^3\text{H} + p \rightarrow {}^4\text{He} + \gamma$	19.81	0.416

TABLE I: Correction from pair production to the thermally averaged rates, at $T_9 = 0.8$.

Even the largest correction in this table is still below the current errors for the corresponding photon emission reaction rates.

III. VACUUM POLARIZATION CORRECTIONS

Vacuum polarisation modifies the Coulomb potential, and this affects how cross-sections are extrapolated in energy when taking into account the Gamow penetration factor. We find that this is relevant for the reaction (1b) and we detail in this section how and when this must be taken into account. We follow Ref. [25] which applied these corrections in the context of solar nuclear reactions.

Let us consider two charged nuclei 1 and 2 with charges Z_1 and Z_2 and reduced mass μ . The Coulomb potential is

$$V_C(r) = \frac{Z_1Z_2e^2}{4\pi r} = \frac{Z_1Z_2\alpha_{\text{FS}}}{r}. \quad (35)$$

The Uehling-Serber potential [36, 37] is an additive correction which takes into account electron vacuum polarisation, that is fermionic loops in the photon propagator. The total potential takes thus the form $V = V_C + V_U$ with

$$V_U(r) = V_C(r) \times \frac{2\alpha_{\text{FS}}}{3\pi} I(r). \quad (36)$$

The Uehling function is given by

$$I(r) \equiv \int_1^\infty e^{-2m_e r x} \left(1 + \frac{1}{2x^2}\right) \frac{\sqrt{x^2 - 1}}{x^2} dx. \quad (37)$$

Usually, nuclear reaction cross sections are proportional to the Gamow penetration factor related to the electrostatic potential, which is

$$\Gamma(E) = \exp \left[-2 \int_{r_{\min}}^b \sqrt{2\mu(V(r) - E)} dr, \quad (38)$$

where b is the turning point defined by the classical barrier $V(b) \equiv E$, that is $b = Z_1 Z_2 \alpha_{\text{FS}} / E$, and r_{\min} is the distance at which nuclear forces overcome the repulsive barrier, typically the sum of the radii of the interacting nuclei.

When considering only the Coulomb potential (35) and setting $r_{\min} = 0$, the penetration factor can be expressed with the Sommerfeld parameter

$$\eta \equiv \frac{Z_1 Z_2 \alpha_{\text{FS}}}{\sqrt{2E/\mu}} \quad (39)$$

since after performing the integral in (38) we get

$$\Gamma(E) = \exp[-2\pi\eta]. \quad (40)$$

In Ref. [25] it is shown that taking into account the Uehling-Serber potential translates into a modification of the Gamow penetration factor by

$$\Gamma_{\text{C+U}}(E) = \Gamma_{\text{C}}(E)[1 - \Delta(E)], \quad (41)$$

where

$$\Delta(E) \equiv \frac{4\alpha_{\text{FS}}\eta}{3\pi} \int_0^1 \frac{I(by)}{\sqrt{y - y^2}} dy. \quad (42)$$

The function $\Delta(E)$ is evaluated by switching the order of integration. The y -integral can be performed analytically, leaving us with one numerical integral over x ,

$$\Delta(E) = \frac{4\alpha_{\text{FS}}\eta}{3\pi} \int_1^\infty J \left(\frac{m_e x Z_1 Z_2 \alpha_{\text{FS}}}{E} \right) \times \left(1 + \frac{1}{2x^2} \right) \frac{\sqrt{x^2 - 1}}{x^2} dx, \quad (43)$$

with the definition in terms of a Bessel function of the first kind $J(z) \equiv \pi I_0(z) \exp(-z)$.

However, one cannot ignore the centrifugal barrier which adds to the effective repulsive potential [38], if the interaction takes place via non-zero orbital angular momentum waves. From Fig. 1 and table 3 of Ref. [27], one infers that it is precisely the case that the $\ell = 1$ wave accounts for approximately 85% of the reaction (1b) at BBN energies. The centrifugal effective potential is

$$V_{\text{cen}} = \frac{\ell(\ell + 1)}{2\mu r^2}, \quad (44)$$

where μ is the reduced mass of the two nuclei interacting. For large nuclei, this extra contribution remains small compared with the pure Coulomb barrier (35) and it is possible to treat it as a perturbation as detailed in section

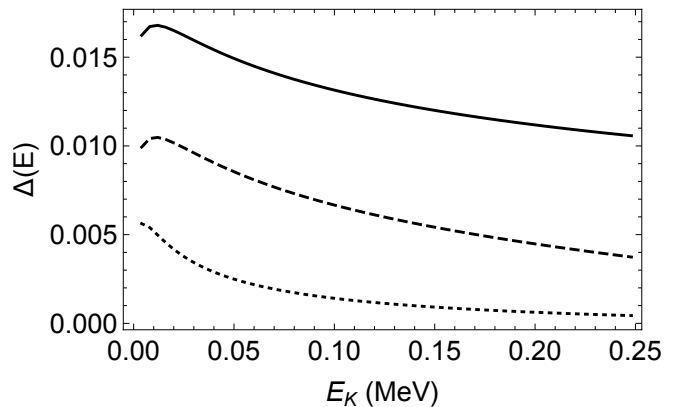


FIG. 3: Relative variation of the Gamow penetration factor $\Delta(E)$ for the reaction (1b) when ignoring the centrifugal barrier ($r_{\min} = 0$ in continuous line and $r_{\min} = 3$ fm in dashed line), and with $\ell = 1$ centrifugal (and also $r_{\min} = 3$ fm) barrier in dotted line.

4.5 of Ref. [38]. However this is not the case for the reaction (1b) at BBN energies and one must in principle estimate the centrifugal barrier directly from $V_C + V_{\text{cen}}$ replaced in (38). The Uehling-Serber potential can still be considered as a perturbation with respect to $V_C + V_{\text{cen}}$, so the correction to the penetration factor, when including the centrifugal barrier, is given by

$$\Delta(E) \equiv \frac{4\alpha_{\text{FS}}\eta}{3\pi} \int_{r_{\min}}^1 \frac{I(by)}{\sqrt{y - y^2 + \frac{\ell(\ell+1)E}{2\mu(Z_1 Z_2 \alpha_{\text{FS}})^2}}} dy. \quad (45)$$

It is not simple to reduce analytically this expression to a one dimensional integral, as was the case without the centrifugal barrier, and we must evaluate numerically directly this two-dimensional integral. The corrections (43) and (45) for the reaction (1b) are plotted on Fig. 3. In the following, we consider only the $\ell = 1$ penetration factor correction from (45) (with $r_{\min} \approx 3$ fm which is roughly the sum of the nuclear radii), that is we ignore the order 15% contribution of the magnetic dipole transition in reaction (1b) at BBN energies.

Cross-sections that are evaluated at energies different from the most likely energy (the Gamow peak), must be extrapolated to the relevant energy range,

$$\sigma_{\text{C+U}}(E) = \sigma_{\text{C}}(E) \frac{[1 - \Delta(E)]}{[1 - \Delta(E_{\text{meas}})]}. \quad (46)$$

The most precise measurement of reaction (1b) was performed at energies smaller than the BBN Gamow peak. Theoretical extrapolations to the BBN energy range was done with the method described in [39], which consists of using mainly the reliable low-energy data [30] and the theoretical model [16]. PRIMAT [10] uses the results of the most recent [40] which implements this type of approach with Bayesian statistics. The energy range of the main source of statistics comes from the measurements of [30] which span $3 \text{ keV} < E_K < 20 \text{ keV}$. On Fig. 3 we

note that this is precisely the range of values for which the function $\Delta(E)$ is nearly constant. Hence we choose to evaluate this function at the value $E_{\text{meas}} = 15$ keV.

To subsequently estimate how this correction affects the thermally averaged rates of reaction (1b), we can evaluate it at the most likely energy (34), so that

$$\frac{\langle[\sigma v]\rangle_{\text{C+U}}}{\langle[\sigma v]\rangle_{\text{C}}} \approx \frac{[1 - \Delta(E_K^{\text{ML}}(T))]}{[1 - \Delta(E_{\text{meas}})]} \approx 1 + \sum_{i=0}^4 b_i T_9^i, \quad (47)$$

where the last equality is a fit with $b_0 = -3.5264 \times 10^{-4}$, $b_1 = 1.4925 \times 10^{-2}$, $b_2 = -2.6236 \times 10^{-2}$, $b_3 = 2.3837 \times 10^{-2}$, $b_4 = -1.0443 \times 10^{-2}$, $b_5 = 1.7473 \times 10^{-3}$ which is valid for $0.05 \leq T_9 \leq 2$. The ratio (47) of the corrected to the uncorrected rates for reaction (1b) is plotted in Fig. 4. Let us emphasize again that we have only performed a

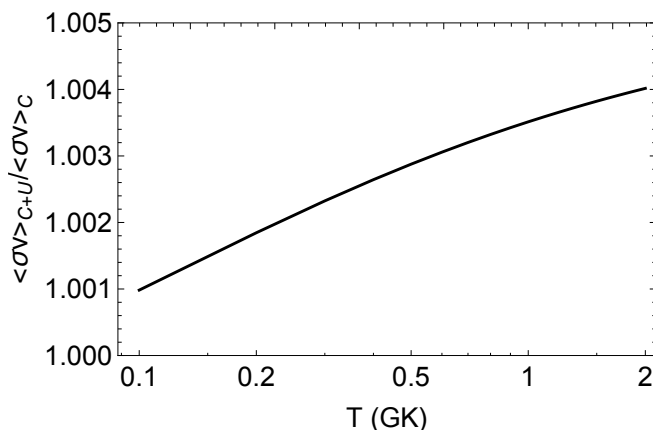


FIG. 4: Corrective ratio $\langle[\sigma v]\rangle_{\text{C+U}}/\langle[\sigma v]\rangle_{\text{C}}$ for the reaction (1b).

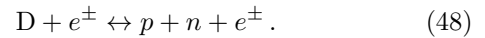
crude estimation of the correction, since once we can use reliable data in the range $E_K = 100 - 200$ keV, as should be available in the future [41], then this correction would no longer need to be taken into account. Alternatively, if the theoretical extrapolation are still used, future precision calculations of the nuclear reaction rates could include the Uehling-Serber correction into account directly in the asymptotics of the Coulomb wave functions.

IV. EFFECT ON BBN

We now review the effect of the corrections discussed in the previous sections on elemental abundances at the end of BBN. For any photon emission reaction, the reverse rate is obtained using detailed balance, as explained in detail in section 4.2 of Ref. [10]. This is also the case for the pair-production reactions since electrons and positrons are always at thermal equilibrium with photons during BBN. Hence one can compute the sum of the photon and pair producing reactions, and then obtain the sum of the backward rates from the very same detailed balance relation. To summarise, if the forward

rate is increased, the backward rate is increased by the same amount so as to always satisfy the detailed balance conditions.

Note that when considering reactions with electron-positron pairs, one should also consider in principle $2 \rightarrow 3$ reactions



These reactions turn out to be negligible for the following reason. The initial electron or positron needs to bring not only the necessary binding energy, but also the final rest mass of the electron or positron. If a photon needs only $E_\gamma = B_D$ to dissociate deuterium, an electron would need $B_D + m_e$. Hence at energies $T \ll m_e$, from the thermal equilibrium distribution of electrons, one deduces that the reaction is suppressed by a factor $\exp(-m_e/T)$ compared with the photon dissociation reaction. Since nucleosynthesis really starts only below $T \approx 100$ keV, this is an additional prohibitive suppression factor. The argument can also be made for the reverse rate, and in that case the suppression factor comes from the low probability of having the three body reaction, since this brings an extra factor $\propto n_e/T^3 \propto \exp(-m_e/T)$.

The effect on BBN of all corrections discussed in the previous is summarised in Table II. Deuterium is by far the most precisely measured component, and we note that in total its predicted abundance is decreased by 0.19%.

Element	Reference	Pair	Pair+Uehling	Tot. Var. %
10^5 D/H	2.4585	2.4564	2.4539	-0.19
10^5 ^3He /H	1.0742	1.0752	1.0763	+0.20
10^{10} ^7Li /H	5.670	5.684	5.695	+0.44

TABLE II: Variations of BBN abundances. The first column gives reference abundances computed with PRIMAT [10]. The second column takes into account the effect of pair production in photon producing processes, and the third column also includes the Uehling potential corrections to reaction (1b). Variation of ^4He is insignificant.

Conclusion

Radiative corrections from pair production have a relative size set by the prefactor α_{FS}/π . In the limit of the energy release being much larger than $2m_e$, the pair-production radiative correction is completely fixed by the photon emission cross section. In reality, this limit does not hold for most of the reactions, and we model the corresponding nuclear EM transition vertex by the simplest electric dipole form. Most of the photon producing reaction rates are indeed dominated by electric dipole transitions, and are easily corrected by a universal function. Synthesis of deuterium is a notable exception, where at lowest energies the reaction is dominated by a magnetic

transition. The reaction $p + D \rightarrow {}^3\text{He} + \gamma$ is also partially determined by the magnetic dipole transition at BBN energies, but we ignored this complication as detailed in section II J, because the relative difference between corrections to magnetic and electric transitions becomes less important as Q is taken to be much larger than $2m_e$. In the limit of zero recoil, we give complete analytic expressions for the pair-production corrections induced by $E1$ and $M1$ nuclear transitions, and correct some mistakes (or typos) in the original reference [21]. Finally, the Uehling-Serber potential creates a finite correction to the Gamow penetration factor, and it needs to be taken into account if the nuclear rates involve extrapolation in energy.

Having evaluated the radiative corrections to nuclear rates, we determine the resulting change in the BBN predictions. The radiative-correction-induced shifts to freeze-out abundances are small, below the percent level, and are summarized in Table II. Nevertheless, expected

progress in CMB physics, observations of deuterium, nuclear physics measurements of the relevant rates, as well as in *ab-initio* calculations of nuclear reactions, may make even sub-percent shifts relevant in the future. The abundance of ${}^4\text{He}$ is very insensitive to the change in nuclear rates, and thus the impact of radiative corrections on helium abundance is negligible.

We thank Alain Coc, Jean-Philippe Uzan and Elisabeth Vangioni for discussions on the topic. CP thanks the Perimeter Institute (Waterloo, Ontario, Canada) and the University of Victoria (British Columbia, Canada), where this work was initiated for the former and completed for the latter. MP is grateful to the groups at IAP and Orsay for kind hospitality. Research at Perimeter Institute is supported by the Government of Canada through Industry Canada and by the Province of Ontario through the Ministry of Economic Development & Innovation.

-
- [1] N. Aghanim et al. (Planck) (2018), 1807.06209.
- [2] R. J. Cooke, M. Pettini, and C. C. Steidel, *Astrophys. J.* **855**, 102 (2018), 1710.11129.
- [3] E. Aver, K. A. Olive, and E. D. Skillman, *JCAP* **7**, 011 (2015), 1503.08146.
- [4] Y. I. Izotov, T. X. Thuan, and N. G. Guseva, *MNRAS* **445**, 778 (2014), 1408.6953.
- [5] D. A. Dicus, E. W. Kolb, A. M. Gleeson, E. C. G. Sudarshan, V. L. Teplitz, and M. S. Turner, *Phys. Rev.* **D26**, 2694 (1982).
- [6] R. E. Lopez, M. S. Turner, and G. Gyuk, *Phys. Rev.* **D56**, 3191 (1997), astro-ph/9703065.
- [7] R. E. Lopez and M. S. Turner, *Phys. Rev.* **D59**, 103502 (1999), astro-ph/9807279.
- [8] L. S. Brown and R. F. Sawyer, *Phys. Rev.* **D63**, 083503 (2001), astro-ph/0006370.
- [9] P. D. Serpico, S. Esposito, F. Iocco, G. Mangano, G. Miele, and O. Pisanti, *JCAP* **0412**, 010 (2004), astro-ph/0408076.
- [10] C. Pitrou, A. Coc, J.-P. Uzan, and E. Vangioni, *Phys. Rept.* **754**, 1 (2018), 1801.08023.
- [11] A. D. Dolgov, S. H. Hansen, and D. V. Semikoz, *Nucl. Phys.* **B503**, 426 (1997), hep-ph/9703315.
- [12] G. Mangano, G. Miele, S. Pastor, and M. Peloso, *Phys. Lett.* **B534**, 8 (2002), astro-ph/0111408.
- [13] G. Mangano, G. Miele, S. Pastor, T. Pinto, O. Pisanti, and P. D. Serpico, *Nucl. Phys.* **B729**, 221 (2005), hep-ph/0506164.
- [14] E. Grohs, G. M. Fuller, C. T. Kishimoto, M. W. Paris, and A. Vlasenko, *Phys. Rev.* **D93**, 083522 (2016), 1512.02205.
- [15] S. Ando, R. H. Cyburt, S. W. Hong, and C. H. Hyun, *Phys. Rev.* **C74**, 025809 (2006), nucl-th/0511074.
- [16] L. E. Marcucci, M. Viviani, R. Schiavilla, A. Kievsky, and S. Rosati, *Phys. Rev.* **C72**, 014001 (2005), nucl-th/0502048.
- [17] K. Arai, S. Aoyama, Y. Suzuki, P. Descouvemont, and D. Baye, *Phys. Rev. Lett.* **107**, 132502 (2011).
- [18] P. Navrátil and S. Quaglioni, *Phys. Rev. Lett.* **108**, 042503 (2012).
- [19] T. Neff, *Phys. Rev. Lett.* **106**, 042502 (2011).
- [20] J. Dohet-Eraly, P. Navrtil, S. Quaglioni, W. Horiuchi, G. Hupin, and F. Raimondi, *Phys. Lett.* **B757**, 430 (2016), 1510.07717.
- [21] N. M. Kroll and W. Wada, *Physical Review* **98**, 1355 (1955).
- [22] L. G. Landsberg, *Phys. Rept.* **128**, 301 (1985).
- [23] H.-J. Assenbaum, K. Langanke, and G. Soff, *Physics Letters B* **208**, 346 (1988).
- [24] D. Trautmann, G. Baur, D. Vetterli, P. Egelhof, R. Henneck, M. Jaskòla, H. Mühry, and I. Sick, *Nuclear Physics A* **533**, 528 (1991).
- [25] M. Kamionkowski and J. N. Bahcall, *Phys. Rev. C* **49**, 545 (1994), astro-ph/9306024.
- [26] V. Berestetskii, L. Landau, E. Lifshitz, L. Pitaevskii, and J. Sykes, *Quantum Electrodynamics*, Course of theoretical physics (Pergamon Press, 1982).
- [27] G. J. Schmid, B. J. Rice, R. M. Chasteler, M. A. Godwin, G. C. Kiang, L. L. Kiang, C. M. Laymon, R. M. Prior, D. R. Tilley, and H. R. Weller, *Phys. Rev. C* **56**, 2565 (1997).
- [28] G. J. Schmid, R. M. Chasteler, C. M. Laymon, H. R. Weller, R. M. Prior, and D. R. Tilley, *Phys. Rev. C* **52**, R1732 (1995).
- [29] L. Ma, H. J. Karwowski, C. R. Brune, Z. Ayer, T. C. Black, J. C. Blackmon, E. J. Ludwig, M. Viviani, A. Kievsky, and R. Schiavilla, *Phys. Rev. C* **55**, 588 (1997).
- [30] C. Casella, H. Costantini, A. Lemut, B. Limata, R. Bonetti, C. Brogini, L. Campajola, P. Corvisiero, J. Cruz, A. D’Onofrio, et al., *Nucl. Phys. A* **706**, 203 (2002).
- [31] R. S. Canon, S. O. Nelson, K. Sabourov, E. Wulf, H. R. Weller, R. M. Prior, M. Spraker, J. H. Kelley, and D. R. Tilley, *Phys. Rev. C* **65**, 044008 (2002).
- [32] C. R. Brune, R. W. Kavanagh, and C. Rolfs, *Phys. Rev. C* **50**, 2205 (1994).
- [33] R. J. deBoer, J. Gres, K. Smith, E. Uberseder, M. Wi-

- escher, A. Kontos, G. Imbriani, A. Di Leva, and F. Strieder, *Phys. Rev.* **C90**, 035804 (2014).
- [34] E. G. Adelberger et al., *Rev. Mod. Phys.* **83**, 195 (2011), 1004.2318.
- [35] C. Angulo, M. Arnould, M. Rayet, P. Descouvemont, D. Baye, C. Leclercq-Willain, A. Coc, S. Barhoumi, P. Aguer, C. Rolfs, et al., *Nuclear Physics A* **656**, 3 (1999).
- [36] R. Serber, *Phys. Rev.* **48**, 49 (1935).
- [37] E. A. Uehling, *Physical Review* **48**, 55 (1935).
- [38] D. D. Clayton, *Principles of stellar evolution and nucleosynthesis* (Chicago: University of Chicago Press, 1983).
- [39] A. Coc, P. Petitjean, J.-P. Uzan, E. Vangioni, P. Descouvemont, C. Iliadis, and R. Longland, *Phys. Rev.* **D92**, 123526 (2015), 1511.03843.
- [40] C. Iliadis, K. S. Anderson, A. Coc, F. X. Timmes, and S. Starrfield, *Astrophys. J.* **831**, 107 (2016), 1608.05853.
- [41] C. Gustavino, in *European Physical Journal Web of Conferences* (2017), vol. 136, p. 01009.